Article

Superconducting YBCO Foams as Trapped Field Magnets

Michael R. Koblischka [1,*], S. Pavan Kumar Naik [1,†], Anjela Koblischka-Veneva [1], Masato Murakami [1], Denis Gokhfeld [2], E. Sudhakar Reddy [3,‡], Georg J. Schmitz [3]

[1] Superconducting Materials Laboratory, Department of Materials Science and Engineering, Shibaura Institute of Technology, Tokyo 135-8548, Japan; spavankumarnaik@yahoo.in (S. P. K. N.); anjela@shibaura-it.ac.jp (A. K.-V.); masatomu@shibaura-it.ac.jp (M. M.)
[2] Kirensky Institute of Physics, Federal Research Center KSC SB RAS, Krasnoyarsk, 660036 Russia; gokhfeld@yandex.ru (D. G.)
[3] ACCESS, Intzestrasse 5, 52072 Aachen, Germany; sudhakar_reddy@raychemrpg.com (E. S. R.); g.schmitz@access-technology.de (G. J. S.)
* Correspondence: m.koblischka@gmail.com or miko@shibaura-it.ac.jp
† Current address: Superconducting Electronics Group, Electronics and Photonics Research Institute, National Institute of Advanced Industrial Science and Technology (AIST) 1-1-1 Central 2, Umezono, Tsukuba, Ibaraki, 305-8568, Japan
‡ Current address: Raychem RPG Pvt Ltd., Namdev Garnet, Aga Abbas Ali Road Off Halasur Road, Bangalore 560042, India

Version January 14, 2019 submitted to Materials

Abstract: Superconducting foams of $YBa_2Cu_3O_y$ (YBCO) are proposed as trapped field magnets or supermagnets. The foams with an open-porous structure are light-weight, mechanically strong and can be prepared in large sample sizes. The trapped field distributions were measured using a scanning Hall probe on various sides of an YBCO foam sample after field-cooling in a magnetic field of 0.5 T produced by a square Nd-Fe-B permanent magnet. The maximum trapped field (TF) measured is about 400 G (77 K) at the bottom of the sample. Several details of the TF distribution, the current flow and possible applicatons of such superconducting foam samples in space applications, e.g., as active elements in flux-pinning docking interfaces (FPDI) or as portable strong magnets to collect debris in space, are outlined.

Keywords: High-T_c superconductors; YBCO; foam; trapped fields; current flow)

1. Introduction

Today, high-T_c superconductor samples are mainly fabricated in three different shapes: wires/tapes, thin films and bulk materials [1–3]. The wires and tapes serve the purpose of energy transport or building of large electromagnets, the thin films cover the needs of superconducting electronics and sensors, and the bulk materials are employed for levitation, in electric motors and generators or as trapped field magnets (superconducting permanent magnets), which can be much stronger as any permanent magnet material. For most applications operating at liquid nitrogen temperature (77 K), $YBa_2Cu_3O_y$ (YBCO) is the material of choice due to its superior properties at elevated temperatures [4].

For building superconducting trapped field (TF) magnets or "supermagnets", a large sample size is required as the maximum trapped field depends on the sample size in contrast to permanent magnets [5,6]. However, to reach large sample sizes is a difficult task as a good texture is essential to enable the flow of strong supercurrents. The necessary oxygenation step when preparing YBCO leads to a phase transformation from tetragonal ($O_{6.5}$) to orthorhombic (O_7). In this step, internal cracking

 doi:10.20944/preprints201901.0174.v1

may occur which limits the reachable sample size [7]. Furthermore, the oxygenation time required to fully oxygenate a large, bulk sample increases tremendously; so necessary oxygenation times of 14 days and more are quite common. Therefore, the samples prepared in this way are costly, and difficult to be handled. Furthermore, magnetostriction plays an important role when trapping large magnetic fields [6]. Due to the forces involved, the superconductor sample may break up, so a reinforcement by steel rings and additional polymer impregnation is required [8–10]. In this way, a record trapped field of 17.6 T at 26 K was reached in the literature, measured in between a stack of two melt-textured superconductor samples with 25 mm diameter.

An alternative preparation route would be very interesting to solve the problems mentioned. A possible way out was attempted several years ago with the preparation of superconducting foams. Polymer, metallic or ceramic foams as nature-inspired bionic materials mimicing the construction elements of biologic load-bearing structures like wood or bones are nowadays used in many places in industry for various tasks, e.g., as energy absorbers in aeronautics or the car industry, as light-weight structural damping material, as filter materials, and others. These uses were recently reviewed in Refs. [11–13]. The open-porous structure allows that metallic layers can be added by electrodeposition to further improve the mechanical strength [14], and the pores may be filled with resins, which could be very important for future TF magnets based on superconducting foams. Furthermore, the foam-type material enables an easy upscaling of the sample size [15].

The YBCO foams were originally intended to be used as fault current limiters [16,17], as the open porous structure of the foam materials enables a very effective cooling process. Liquid nitrogen or any other coolant in form of liquid or gas can be sent directly through the sample. Therefore, possible hotspots in the material can be effectively cooled down again [11]. This very effective cooling can be easily demonstrated when cooling a foam sample in liquid nitrogen to perform, e.g., levitation experiments as shown in the Supplementary Materials. The superconducting foams can be applied as trapped field magnets, as the easy upscaling enables to create foam samples of larger dimensions as the conventional bulk samples, avoiding the extremely long oxygenation times required. Furthermore, the foams have much less weight compared to the bulks, and less material is required which also reduces the costs of a sample. These advantages make the superconducting foams ideal candidates for applications in space. This may comprise the flux-pinning docking interfaces (FPDI) discussed in the literature [18,19] and portable high-magnetic field units which can be mounted in satellites to magnetically collect waste debris [20–22].

In this contribution, we present the results of trapped field measurements at 77 K on superconducting YBCO foam materials and discuss the possible applications of such systems.

2. Experimental procedures

The foam samples were prepared at RWTH Aachen, which is described in detail in Refs. [16,17]. Starting from a polyurethane foam, a preform Y_2BaCuO_5 (211) foam was created by filling a 211 slurry into the foam and subsequent sintering to burn off the polyurethane and forming a stable 211 structure. Such a 211 foam is presented in Fig. 1 (a). Figure 1 (b) gives a SEM image of the 3D-structure of the 211 foam, which is a copy of the structure of the original polyurethane foam. The next step of preparation is a transformation of the 211 foam into a superconducting YBCO foam. Here it is important to point out that crystallographic orientation was introduced to the foam by using the infiltration growth process together with a seed crystal on top of the foam structure. This is illustrated in Fig. 1 (c), showing a superconducting YBCO foam with a remnant of the seed crystal on top. This treatment introduced indeed a texture as evidenced by x-ray and neutron diffraction [23]. The superconducting transition temperature, T_c, of the foam samples is 91.1 K like in the bulk samples.

Magnetic measurements were carried out using SQUID magnetometry, for details see, e.g., Ref. [24]. The critical current densities were obtained from the magnetization data using the critical state model [25,26]. Trapped field (TF) measurement of the foam were carried out using a homemade setup with a scanning Hall probe operating at 77 K. The foam sample was field cooled (FC) in a field of

Preprints (www.preprints.org) | NOT PEER-REVIEWED | Posted: 17 January 2019 doi:10.20944/preprints201901.0174.v1

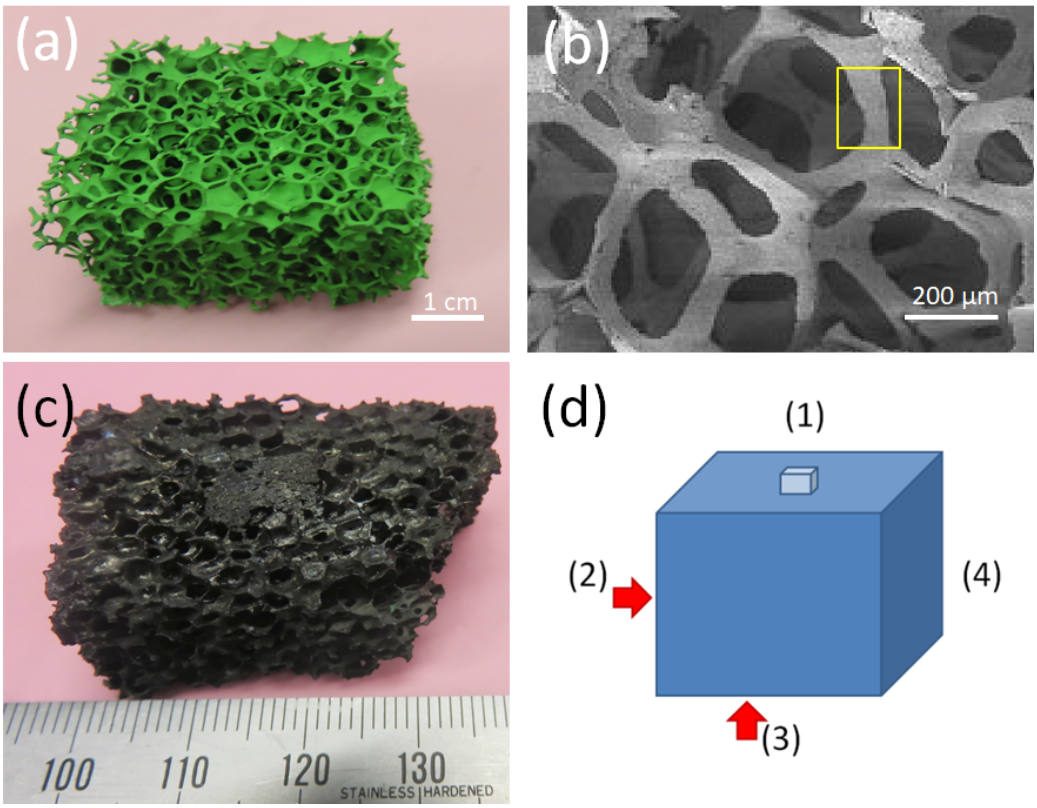

Figure 1. (a) Image of the preform, a green 211 foam, and (b) SEM image of the 3D structure of the 211 foam. The yellow rectangle marks the central piece of a strut as analyzed by magnetic measurements and for the microstructure investigation. (c) presents the fully reacted, superconducting foam. On the top side (1), the seed crystal and a cloth are still visible. (d) gives a schematic drawing of the foam sample and the nomenclature of the sample sides.

a Nd-Fe-B permanent magnet (0.5 T surface field) in liquid nitrogen. For each measurement in this paper, the permanent was placed above the side analyzed. TF flux density profiles were recorded after 15 min waiting time at 1.5 – 2 mm height above the foam surface as the surface of the foam is not fully flat, and no surface treatment was carried out. Therefore, the obtained TF values are slightly smaller than that of other melt-textured bulk samples. The microstructure investigations were performed using scanning electron microscopy (SEM), atomic force microscopy (AFM), and electron backscatter diffraction (EBSD). More details about these measurements can be found in previous publications [27,28].

3. Results and discussion

The foam sample investigated here is presented in Fig. 1 (c). The size of the sample is 5 × 2 × 2 cm^3. Figure 1 (d) presents a schematic drawing of the sample with the nomenclature of the sample sides: The side with the former seed crystal is labelled (1), and then we proceed by turning the sample clockwise by 90°, so that side (2) faces to the top; side (3) corresponds to the bottom side (where still some traces of the former liquid source can be found), and sides (2) and (4) are the short sides of the foam sample. This way of measurement was chosen to see which sample side gives the best TF properties, whereas former TF experiments on foam samples only considered side (1), in analogy to the conventional bulk samples [29].

Figures 2 and 3 show the results of a trapped field experiment on the YBCO foam sample. Field-cooling (FC) was performed in the field of a square Nd-Fe-B magnet which had a surface field

Preprints (www.preprints.org) | NOT PEER-REVIEWED | Posted: 17 January 2019 doi:10.20944/preprints201901.0174.v1

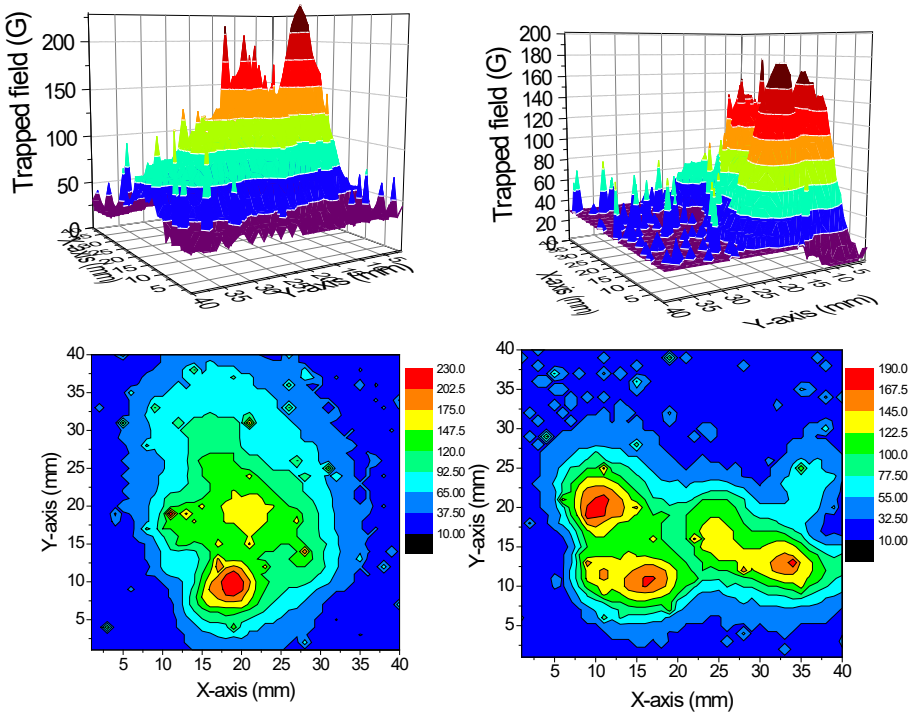

Figure 2. Trapped field measurements on a foam sample. Distribution of B_z measured by scanning Hall probe on the sample sides (1) and (2) of the foam as surface plots (top) and contour plots (bottom). The permanent magnet in the FC cooling process was placed on each side in a separate measurement run.

of 0.5 T (remanent magnetization 1.3 T). For each measurement, the magnet was placed above the investigated sample side, and field-cooling was performed in this way.

Figure 2 gives the measured trapped field distributions as 3D surface plots as well as contour plot for the foam sample surface (1) and the side (2), and Fig. 3 shows the measurement results for sides (3) and (4). On all sample sides, we find a large trapped field peak, and characteristically, also the presence of several sharp, small peaks. The foam sides (1) and (2) exhibit several smaller peaks with only a small value of B_{trap}, whereas the sides (3) and (4) show broad TF peaks. On side (4), the maximum trapped field of 400 G is recorded. This is a surprising result, as we would have expected the maximum trapped field either on side (1) or on side (3), as position-dependent measurements of the properties of foam struts had shown increasing j_c towards the bottom of the foam sample [30]. Remarkably, there are many of the small, sharp peaks especially on side (3), the bottom side of the foam sample.

The TF measurements clearly demonstrate the presence of two types of currents in the foam sample – one current density, which is running through the entire sample perimeter, resulting in the large, cone-shaped maxima with $B_{\mathrm{trap,max}}$, and one locally distributed current density being responsible for the small, sharp peaks. Both currents are percolative, truely 3D currents flowing through the foam struts, and are not confined to planes in the sample. Repeating the scan of B_z reproduces most of these peaks, but the height may vary. We ascribe these peaks to local current loops in the sample, which were formed around local defects (e.g., large pores, pore clusters or non-superconducting struts), and are compressed due to the rearrangement of the internal field, B_i, when removing the external field. Similar observations were made already in Ref. [29], where only the surface (1) close to the seed crystal was measured. Here we have to note that the Hall probes measure only the z-component of B, which implies that current paths along the z-axis without a z-component of the generated magnetic field will

Preprints (www.preprints.org) | NOT PEER-REVIEWED | Posted: 17 January 2019 doi:10.20944/preprints201901.0174.v1

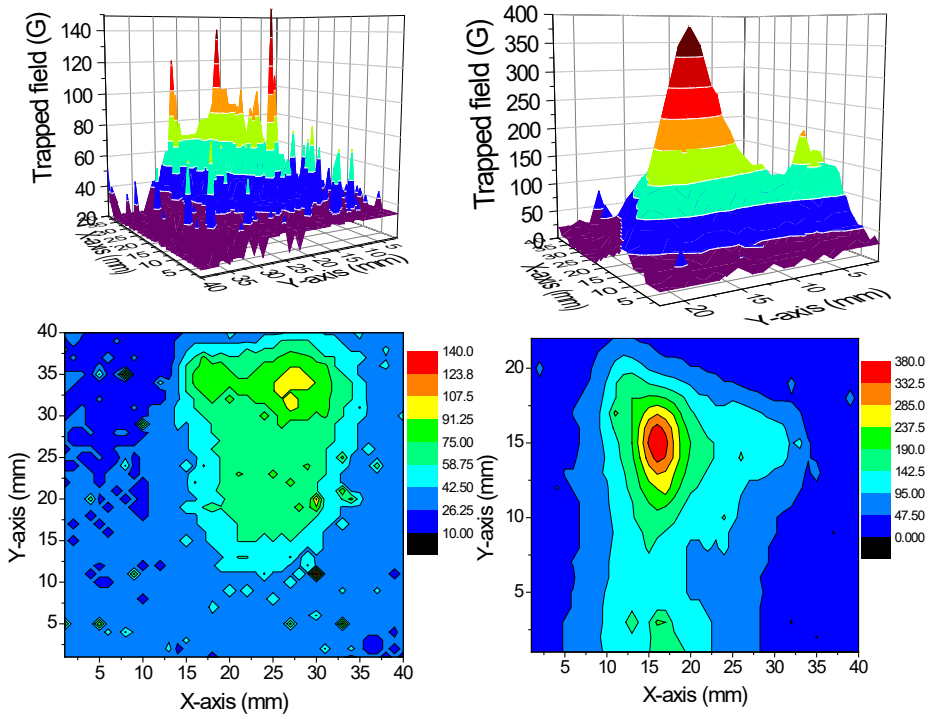

Figure 3. Trapped field measurements on a foam sample. Distribution of B_z measured by scanning Hall probe on the sample sides (3) and (4) of the foam as surface plots (top) and contour plots (bottom).

not be detected. Only the *(a,b)*-projection of the real circulating 3D currents will be measured, and, the various contributions to it are weighted relative to their distance to the scanning Hall probes.

The present trapped field values recorded are not spectacular, as the values are still much smaller than those obtained on YBCO or GdBCO bulk samples at 77 K. The current records are about 800 mT (SmBCO) and 1.1 T (GdBCO) when cooling the sample to 77 K in 1.3/1.6 T applied magnetic field [31,32]. But here it is important to mention that the current shape of the foams was never optimized to reach large trapped fields, nor the texture of the sample is fully optimized. A dominating orientation like the conventional bulk samples in *c*-direction is reached, but magnetization measurements even on single struts still reveal signs of granularity [33]. The first TF experiments on foams carried out in 2003 [29] had shown trapped fields of ∼400 G, when field-cooling the foam sample in a field of 600 mT on side (1) only. In these experiments, it was noted that a broad TF peak and several sharp peaks resulted. As already mentioned, the trapped field values measured here are still smaller than those of conventional YBCO bulks, but regarding the difference in current density, the porosity and the reduced weight of the foam samples, the results obtained are quite reasonable. Also, most IG-processed bulks are even currently found to exhibit still smaller trapped fields as the melt-textured, melt-growth-processed YBCO bulks [34]. Furthermore, the present foam sample is now already 15 years old and has underwent many experiments as shown in Fig. 6 below.

A simple estimation of the overall transport current density in the foam sample can be done using the size of the trapped field peak (B_{trap}) with the relation [25]

$$J_c R \propto B_{\mathrm{trap}}/\mu_0 \quad . \tag{1}$$

With a trapped field of 250 G and $R = 15$ mm, we obtain $J_c = 130$ A/cm^2; and for the maximum trapped field of 400 G, we have $R = 5$ mm, so $J_c = 630$ A/cm^2.

Preprints (www.preprints.org) | NOT PEER-REVIEWED | Posted: 17 January 2019 doi:10.20944/preprints201901.0174.v1

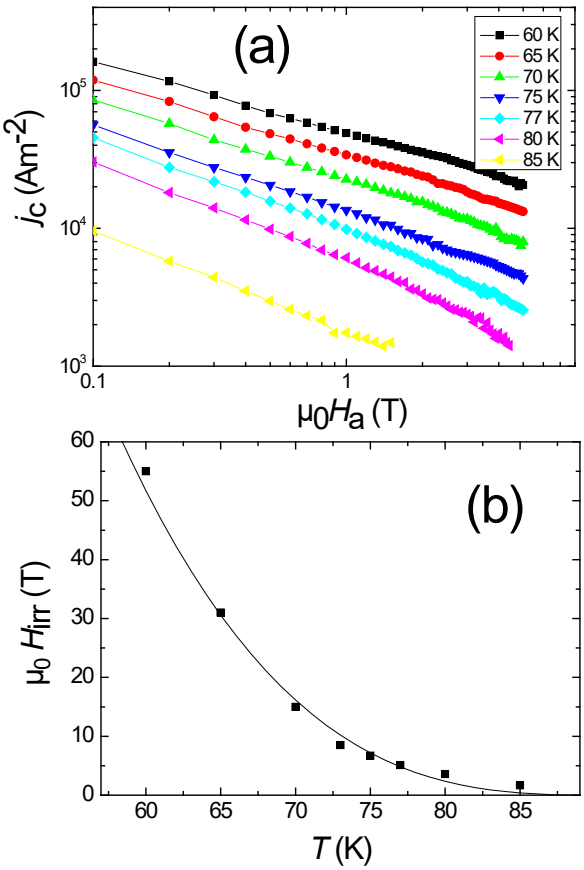

Figure 4. (a) Critical current density, j_c, measured on a single foam strut piece, and irreversibility field, H_{irr} as function of temperature (b). The solid line is a fit using the relation $H_{\mathrm{irr}} = H_{\mathrm{irr}}(0)(1 - T/T_c)^n$ with $n = 3$, common for many 123-materials [35].

Due to the multi-peak trapped field distribution as seen in Figs. 2 and 3, this estimation gives the lower boundary for the real critical current density flowing in the sample. This observation points out that the current flow in such porous samples is more complex as in bulk samples, so we need a closer look to it. Concerning the current flow in porous high-T_c materials, we have to be aware that these are polycrystalline materials, so that we have to consider two different contributions to j_c; the intergranular ($j_{\mathrm{c,inter}}$) and intragranular ($j_{\mathrm{c,intra}}$) currents. The intragranular currents are controlled by the flux pinning and are as high as those of single crystals or bulk samples, whereas the intergranular currents are affected by the grain boundaries between the superconducting grains and by the relative orientations of the anisotropic granules to each other. This describes the case of dense, bulk polycrystalline samples. In porous samples, there is an additional contribution due to the percolative current flow caused by the porosity and the spacial orientation of the foam struts to the external field. Therefore, the overall currents flowing through the entire sample are limited by all these factors, which is the main drawback for all kinds of porous superconducting materials produced so far [36–40].

Figure 4 (a) gives a double log-plot of the critical current density, j_c, measured on a piece of a foam strut (see the yellow rectangle in Fig. 1 (b)). This current density represents an intragranular current density. The $j_c(H)$ curves in this plot look nearly linear, and do not show any so-called fishtail effect [41]. The curves can be fitted using a power law, $H^{-\alpha}$ with α ranging between $\sim$0.52 (60 K) and 0.8 (85 K). The values of α are simillar to ones obtained on YBCO coated conductors [42], indicating dominant weak collective flux pinning.

Preprints (www.preprints.org) | NOT PEER-REVIEWED | Posted: 17 January 2019 doi:10.20944/preprints201901.0174.v1

Bending down of the curves at high H and high T is due to thermal activation. Also, to further interpret these data, the knowledge about the microstructure of such a foam strut is essential.

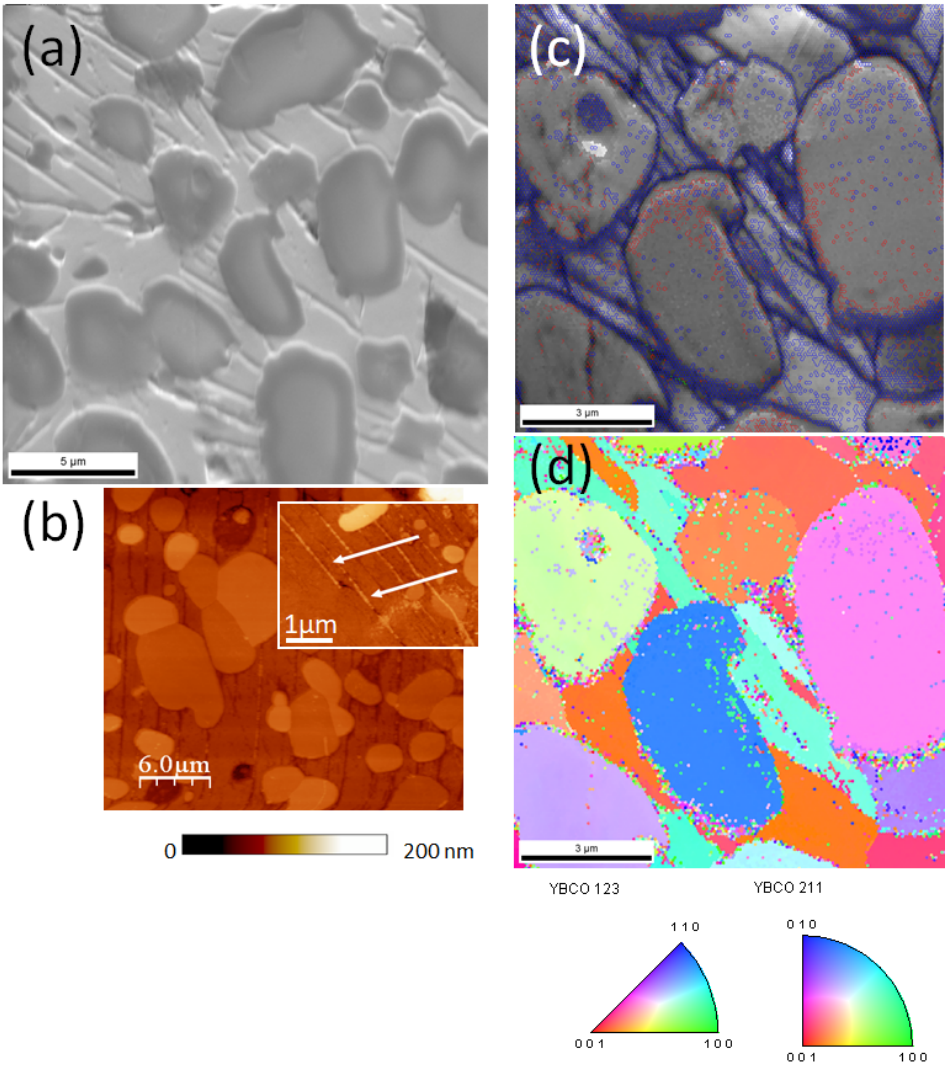

Figure 5. Microstructure of a foam strut piece, investigated by SEM (a), AFM topography (b) and EBSD (c, d). (c) gives an image quality map, together with the EBSD-detected grain boundaries colored in (1–5° misorientation), green (5–15° misorientation) and blue (15–180° misorientation). (d) shows an orientation map in [001]-direction. The color code is given in the stereographic triangles below the map. The YBCO matrix shows two dominating orientations, whereas the 211 particles (both large and tiny ones) are randomly oriented.

The YBCO foam shows much higher values of the irreversibility field, H_{irr}, as presented in Fig. 4 (b). $H_{irr}(T)$ values were determined from the closing of the magnetization loops, and for temperatures, where this was not possible, the H_{irr} values were determined via the flux pinning force scaling as described in detail in Ref. [33]. The values of H_{irr} are clearly much higher than those of other YBCO superconductors, being comparable to those of IG-processed, YBCO bulk samples [43,44]. The H_{irr} reaches 7 T already at 77 K, which renders the measurement already difficult using the normal laboratory equipment [33]. The irreversibility field is known to be strongly dependent on the pinning strength and on the scale of the current circulation [45,46]. As also texture is achieved in the YBCO foam samples [36], this is very promising for future improvement of the overall critical current densites of such foam samples.

Preprints (www.preprints.org) | NOT PEER-REVIEWED | Posted: 17 January 2019 doi:10.20944/preprints201901.0174.v1

For achieving high critical current densities in YBCO foam samples, the texture is essential as the grain boundaries in a polycrystalline material will limit the possible current flow [1]. Therefore, it is important to investigate the microstructure of the foam struts as shown in Fig. 5. Figure 5 (a) gives a backscattered electron image of a mechanically polished foam strut piece. Here, we can see several large 211 grains embedded in the superconducting YBCO matrix. This matrix shows several characteristic stripes, which are due to either grain boundaries or sub-grain boundaries. In Fig. 5 (b), an AFM topography scan is presented. Here, the mechanically harder 211 particles are more clearly visible, and at higher magnification (inset), we can see a large amount of very tiny 211 particles located within the stripes (arrows). Figures 5 (c) and (d) give finally EBSD mappings of a small section of the strut. Figure 5 (c) is an image quality (IQ) map (which resembles a backscattered electron image), together with the EBSD-detected grain boundaries (GBs) drawn in red (1–5° misorientation), green (5–15° misorientation) and blue (15–180° misorientation). The majority of the detected GBs are high-angle GBs, mostly located in the stripes and around the tiny 211 particles. This implies that the current flow through these GBs is somewhat hindered, as a more single-crystalline orientation of the YBCO matrix would allow much higher currents to flow unaltered. On the other hand, the tiny 211 particles are excellent flux pinning sites, so the foam material benefits of their presence, resulting in the improved irreversibility fields as seen in Fig. 4.

Figure 5 (d) shows an orientation map in [001]-direction, i.e., perpendicular to the sample surface. The color code is given in the stereographic triangles below the map. The YBCO matrix shows two dominating orientations (±30° off the (001)-direction (red)). In contrast to this, the 211 particles (both large and tiny ones) are randomly oriented. This observation implies that the foam strut shows a texture, but due to the spacial orientation of the strut within the foam sample, the measured orientation cannot be in (001)-direction as in a conventional bulk sample. Therefore, the currents flowing through a strut face the GBs, which will limit the maximal currents. Thus, the currents measured by magnetization measurements are lower than those of bulk samples [33]. The improvement of this will be the main challenge for the future development of the superconducting foam samples.

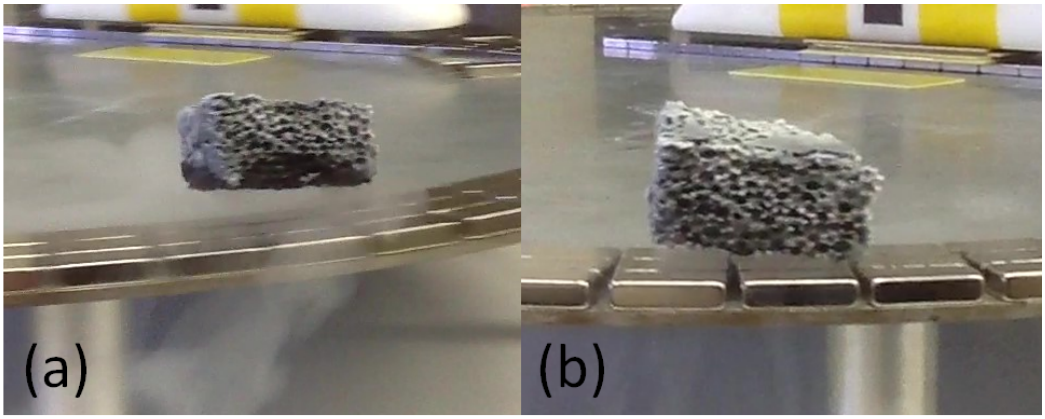

Figure 6. Superconducting foam levitating above a magnetic rail. (a) shows the foam sample at full speed running on the rail, and (b) gives the foam sample when being close to warm up.

Nevertheless, our first results are promising, so thus we may discuss possible applications of the foam samples to set directions and goals for the coming improvements.

The superconducting YBCO foams could see many different applications which make use of the efficient cooling process, e.g., for fault current limiters, which was already discussed in the first publications on foams [16,17]. Cooling of superconducting foam structures from room temperature to 77 K proceeds about ten times faster compared to respective bulk materials of the same mass and composition [11]. This can directly be demonstrated when cooling a foam sample in liquid nitrogen, e.g., to test the levitation properties on a magnetic rail consisting of 3 Nd-Fe-B magnets in a row (S-N-S configuration, [47]) as shown in Fig. 6 and in the video sequence in the Supplementary Materials.

Preprints (www.preprints.org) | NOT PEER-REVIEWED | Posted: 17 January 2019 doi:10.20944/preprints201901.0174.v1

When operating on such a magnetic rail, the foam sample is cooled so well that it takes ∼5 min to warm up again. Furthermore, the lift height of the foam sample is much higher than that of an YBCO bulk sample due to the reduced weight. Another interesting possibility would be to turn around the situation of the levitation experiment: Using long pieces of foam would create an easily coolable superconducting rail, where magnetic objects can levitate upon. Such a superconducting rail system could be cooled very effectively by any gaseous or liquid coolant being pumped through.

Trapped field magnets can be sources of magnetic fields in places where the standard technology to generate large magnetic fields will not work. Such examples are:
(i) The TF magnets can be applied as static or rotating elements in electric motors and generators (see e.g., the review in Ref. [48]). Here, the reduced weight of the foam samples is very promising. This also applies for another application as magnetic coupling elements in the power line, which is employed to transmit power into a container with different atmospheric conditions. Such light-weight machinery and coupling elements may be useful for space applications.
(ii) TF magnets are portable systems. As long as the system is kept below the superconducting transition temperature, T_c, the magnetic field will stay in the sample. Using the persistent current mode, there is no need for any power supply.
(iii) Combined with pulsed magnetic fields (PFM) [49,50], the superconducting samples can be activated as TF magnets at wish, or serve as field receptors when only being cooled.

The points presented here set the possible uses for light-weight TF magnets, but are not yet all application possibilities for superconducting foam samples. Superconducting foams with small open porosity can easily be continuously reinforced, e.g. with resins, to improve their mechanical properties and, thus, to overcome the forces encountered in levitation and quasi-permanent magnet applications [8]. Also an electroplating process to further improve the mechanical strength as done for metallic Al foams [14] could be carried out here. This will avoid the cracking problems of bulk superconductor samples prevailing when trapping large magnetic fields at low temperatures. All these improvements can be applied to the YBCO foam samples, which will contribute to bring these applications to reality.

Two main applications of superconducting foam samples in space engineering can be envisaged: The foam samples may play an important role for the pinning force docking interfaces (FPDI) discussed in Refs. [18,19]. The supercoducting material required in this application needs to be of large size, i.e., several centimeters in diameter. This size is still out-of-reach for conventional bulk samples, and the weight of such a sample will be considerable, and cracking of the sample may be an important issue. The FPDI system makes use of the stiff field-trapping capability of the superconducting material. One satellite would be equipped with a permanent magnet, and the other one with a superconducting element including a cryocooler. This approach will clearly simplify the docking process between two spacecrafts.

The other space application would be the collection of waste debris in space [20–22] using a large magnetic field. The required system could be integrated in a satellite when using a superconducting TF magnet. A cryocooler would keep the superconducting sample at the required temperature to maintain the magnetic field. If not needed anymore, the sample may warm up above T_c and the system is demagnetized. To switch on again, a PFM pulse may be employed. In this way, the system is capable to be swtiched on and off on demand.

The large amount of possible applications of foam samples suggest that further development of this sample type is an important task for the future. Combining the latest developments concerning the IG-processing of HTSc materials, the newly developed large seed crystals, the optimization of the sample shape for the given task and improved understanding of the open porous structure via extensive modelling of the 3D structure [51,52] can lead to unique types of superconducting samples to fulfill different demands of applications.

4. Conclusions

To conclude, porous high-T_c superconductors are very promising materials for applications whereever the sample weight or the cooling efficiency counts. This is given, e.g., in space experiments, for fault current limiters, and trapped field applications in rotating machinery. The achieved trapped field values are still small, but promising and the cooling efficiency can be demonstrated in simple levitation experiments. The future work will require also a deeper understanding of the current flow in such samples, combining already existing modelling approaches of mechanical properties of metallic foams with modelling of the superconducting current flow. Thus, the superconducting foams may be a handy way to generate large magnetic fields in space.

Supplementary Materials: The following are available online at http://www.mdpi.com/1996-1944/xx/1/5/s1, Video S1: Demonstration of levitating foam sample.

Author Contributions: M. R. K. designed the study, analyzed the data and wrote the paper; S. P. K. N. performed the trapped field measurements; A. K.-V. performed the EBSD analysis; M. M. advised the research; D. G. worked on the data analysis and the current flow; E. S. R. and G. J. S. prepared the foam sample. All authors discussed and approved the final manuscript.

Funding: This work is part of the SUPERFOAM international project funded by ANR and DFG under the references ANR-17-CE05-0030 and DFG-ANR Ko2323-10, respectively. Further funding by a SIT start-up grant is also gratefully acknowledged.

Acknowledgments: We thank K. Berger, B. Douine and Q. Nouailhetas (GREEN, Nancy, France) for valuable discussions concerning applications of the superconducting foam materials. M.R.K. would like to acknowledge inspiring discussions with the late Prof. Roeser (IRS Stuttgart, Germany), who was very enthusiastic about possible applications of the superconducting foams in satellites when I had presented this work to him in a seminar at IRS. This work is, therefore, dedicated to him.

Conflicts of Interest: The authors declare no conflict of interest.

References

1. Larbalestier, D. C., Gurevich, A., Feldmann, D. M., Polyanskii, A. High-T_c superconducting materials for electric power applications. *Nature* **2001**, *414*, 368–377.
2. Eisterer, M., Moon, S. H., Freyhardt, H. C. Current developments in HTSC coated conductors for applications. *Supercond. Sci. Technol.* **2016**, *29*, 060301.
3. Durrell, J. H., Ainslie, M. D.. Zhou, D., Vanderbemden, P., Bradshaw, T., Speller, S., Filipenko, M., Cardwell, D. A. Bulk superconductors: A roadmap to applications. *Supercond. Sci. Technol.* **2018**, *31*, 103501.
4. Gurevich, A. To use or not to use cool superconductors. *Nature Mater.* **2011**, *10* 255-259.
5. Tournier, R., Beaugnon, E., Belmont, O. Processing of large $Y_1Ba_2Cu_3O_{7-x}$ single domains for current-limiting applications. *Supercond. Sci. Tech.* **2000**, *13*, 886–896.
6. Johansen, T. H. Flux-pinning-induced stress and magnetostriction in bulk superconductors. *Supercond. Sci. Technol.* **2000**, *13*, R121–R137.
7. Diko, P. Cracking in melt-grown RE-Ba-Cu-O single-grain bulk superconductors. *Supercond. Sci. Technol.* **2004**, *17*, R45–R58.
8. Tomita, M., Murakami, M. High-temperature superconductor bulk magnets that can trap magnetic fields above 17 tesla at 29 K. *Nature* **2003**, *421*, 517–520.
9. Durrell, J. H., Dennis, A. R., Jaroszynski, J., Ainslie, M. D., Palmer, K. G. B., Shi, Y.-H., Campbell, A. M., Hull, J., Strasik, M., Hellstrom, E. E., Cardwell, D. A. A trapped field of 17.6 T in melt-processed bulk Gd-Ba-Cu-O reinforced with shrink-fit steel. *Supercond. Sci. Tech.* **2014**, *27*, 082001.
10. Vakaliuk, O. I., Ainslie, M. D., Halbedel, B. Lorentz force velocimetry using a bulk HTS magnet system: proof-of-concept. *Supercond. Sci. Technol.* **2018**, *31*, 084003.
11. Nettleship, I. Applications of porous ceramics. *Key Eng. Mater.* **1996**, *122*, 305–324.
12. Colombo, P. Ceramic foams: fabrication, properties and applications. *Key Eng. Mater.* **2002**, *206-213*, 1913–1918.
13. Hill, Ch., Eastoe, J. Foams: From nature to industry. *Adv. Colloid Interface Sci.* **2017**, *247*, 496–513.

14. Jung, A., Diebels, S., Koblischka-Veneva, A., Schmauch, J., Barnoush, A., Koblischka, M. R. Microstructural analysis of electrochemical coated open-cell metal foams by EBSD and nanoindentation. *Adv. Eng. Mater.* **2013**, *16*, 15–20.
15. Noudem, J. G. Developing of shaping textured superconductors. *J. Supercond.* **2011**, *24*, 105–110.
16. Reddy, E. S. Schmitz, G. J. Superconducting foams. *Supercond. Sci. Technol.* **2002**, *15*, L21–L24.
17. Reddy, E. S., Schmitz, G. J. Ceramic foams. *Am. Ceram. Soc. Bull.* **2002**, *81*, 35–37.
18. Shoer, J., Wilson, W., Jones, L., Knobel, M., Peck, M. Microgravity Demonstrations of Flux Pinning for Station-Keeping and Reconfiguration of CubeSat-Sized Spacecraft *J. Spacecraft Rockets* **2010**, *47*, 1066-1069.
19. Yang, W., Liao, D., Yao, L. Effects of magnetization conditions on dynamic characteristics of spacecrafts with superconducting flux pinning docking interfaces. *J. Appl. Phys.* **2018**, *124*, 213901.
20. Nicholas L. Johnson, E. Stansbery, J.-C. Liou, M. Horstman, C. Stokely, D. Whitlock The characteristics and consequences of the break-up of the Fengyun-1C spacecraft. *Acta Astronautica* **2008** *63*, 128-135.
21. A. Giffin, M. N. Shneider, and R. B. Miles Potential micrometeoroid and orbital debris protection system using a gradient magnetic field and magnetic flux compression. *Appl. Phys. Lett.* **2010**, *97*, 054102.
22. Zheng, F. Model for Choosing Best Alternative to Remove Space Junk. *Adv. Eng. Res. (AER)*, **2017**, *130*, 1067-1070.
23. Noudem, J. G., Guilmeau, E., Chateigner, D., Lambert, S., Reddy, E. S., Ouladdiaf, B., Schmitz, G. J. Properties of $YBa_2Cu_3O_y$-textured superconductor foams. *Physica* C **2003**, *408–410* 655–656.
24. Zeng, X. L., Karwoth, T., Koblischka, M. R., Hartmann, U., Gokhfeld, D., Chang, C., Hauet, T. Analysis of magnetization loops of electrospun nonwoven superconducting fabrics. *Phys. Rev. Mater.* **2017**, *1*, 044802.
25. Bean, C. P. Magnetization of hard superconductors. *Phys. Rev. Lett.* **1962**, *8*, 250–253.
26. Chen, D. X., Goldfarb, R. B. Kim model for the magnetization of hard superconductors. *J. Appl. Phys.* **1989**, *66*, 2489–2500.
27. Koblischka, M. R., Koblischka-Veneva, A., Reddy, E. S., Schmitz, G. J. Analysis of the microstructure of superconducting YBCO foams by means of AFM and EBSD. *J. Adv. Ceram.* **2014**, *3*, 317–325.
28. Koblischka-Veneva, A., Koblischka, M. R., Ide, N., Inoue, K., Muralidhar, M., Hauet, T., Murakami, M. Microstructural and magnetic analysis of a superconducting foam and comparison with IG-processed bulk samples. *J. Phys. Conf. Ser.* **2016**, *695*, 012002.
29. Bartolomé, E., Granados, X., Puig, T., Obradors, X., Reddy, E. S., Schmitz, G. J. Critical state in superconducting single-crystalline $YBa_2Cu_3O_7$ foams: Local versus long-range currents. *Phys. Rev.* B **2004**, *70*, 144514.
30. Koblischka, M. R., Koblischka-Veneva, A., Berger, K., Nouailhetas, Q., Douine, B., Reddy, E. S., Schmitz, G. J. Current flow and flux pinning properties of YBCO foam struts. *IEEE Trans. Appl. Supercond.*, submitted for publication.
31. Wang, Y.-N., Yang, W.-M., Yang, P.-T., Zhang, Ch.-Y., Chen, J.-L., Zhang, L.-J., Chen, L. Influence of trapped field on the levitation force of SmBCO bulk superconductor. *Physica* C **2017**, *542*, 28–33.
32. D. A. Zhou, D., Shi, Y., Zhao, W., Dennis, A. R., Beck, M., Ainslie, M. D., Palmer, K. G. B., Cardwell, D. A., Durrell, J. H. Full Magnetization of Bulk (RE)$Ba_2Cu_3O_{7-\delta}$ Magnets With Various Rare-Earth Elements Using Pulsed Fields at 77 K. *IEEE Trans. Appl. Supercond.* **2017**, *27*, 6800704.
33. Koblischka, M. R., Koblischka-Veneva, A., Chang, C., Hauet, T., Reddy, E. S., Schmitz, G. J. Flux pinning analysis of superconducting YBCO foam struts. *IEEE Trans. Appl. Supercond.* DOI: 10.1109/TASC.2018.2880334.
34. Namburi, D. K., Durrell, J. H., Jaroszynski, J., Shi, Y., Ainslie, M. D., Huang, K., Dennis, A. R., Hellstrom, E. E., Cardwell, D. A. A trapped field of 14.3 T in Y-Ba-Cu-O bulk superconductors fabricated by buffer-assisted seeded infiltration and growth. *Supercond. Sci. Technol.* **2018**, *31* 125004.
35. Altin, E., Gokhfeld, D. M., Demirel, S., Oz, E., Kurt, F., Altin, S., Yakinci, M. E. Vortex pinning and magnetic peak effect in Eu(Eu,Ba)$_{2.125}Cu_3O_x$. *J. Mater. Sci.: Mater. Electron.* **2014**, *25*, 1466-1473.
36. Noudem, J. G., Reddy, E. S., Schmitz, G. J. Magnetic and transport properties of $YBa_2Cu_3O_y$ superconductor foams. *Physica* C **2002**, *390*, 286–290.
37. Petrov, M. I., Tetyueva, T. N., Kveglis, L. I., Efremov, A. A., Zeer, G. M., Shaikhutdinov, K. A., Balaev, D. A., Popkov, S. I., Ovchinnikov, S. G. Synthesis, Microstructure, and the Transport and Magnetic Properties of Bi-Containing High-Temperature Superconductors with a Porous Structure. *Tech. Phys. Lett.* **2003**, *29*, 986–988.

 doi:10.20944/preprints201901.0174.v1

38. Fiertek, P., Sadowski, W. Processing of porous structures of $YBa_2Cu_3O_{7-\delta}$ high-temperature superconductor. *Material Science Poland* **2006**, *24*, 1103–1108.
39. Fiertek, P., Andrzejewski, B., Sadowski, W. Synthesis and transport properties of porous superconducting ceramics of $YBa_2Cu_3O_{7-\delta}$. *Rev. Adv. Mater. Sci.* **2010**, *23*, 52–56.
40. Koblischka, M. R., Koblischka-Veneva, A. Porous high-T_c superconductors and their applications. *AIMS Material Sci.* **2018**, *5*, 1199–1213.
41. Jirsa, M., Půst, L., Dlouhý, D., Koblischka, M. R. Fishtail shape in the magnetic hysteresis loop for superconductors: Interplay between different pinning mechanisms. *Phys. Rev.* B **1997**, *55*, 3276–3284.
42. Polat, Ö., Sinclair, J. W., Zuev, Y. L., Thompson, J. R., Christen, D. K., Cook, S. W., Kumar, D., Chen, Y., Selvamanickam, V. Thickness dependence of magnetic relaxation and $E - J$ characteristics in superconducting Gd-Y-Ba-Cu-O films with strong vortex pinning. *Phys. Rev.* B **2011**, *84*, 024519.
43. Iida, K., Babu, N. H., Shi, Y., Cardwell, D. A. Seeded infiltration and growth of large, single domain Y-Ba-Cu-O bulk superconductors with very high critical current densities. *Supercond. Sci. Technol.* **2005**, *18*, 1421–1427.
44. Kumar, N. D., Rajasekharan, T., Muraleedharan, K., Banerjee, A., Seshubai, V. Unprecedented current density to high fields in $YBa_2Cu_3O_{7-\delta}$ superconductor through nano-defects generated by preform optimization in infiltration growth process. *Supercond. Sci. Technol.* **2010**, *23*, 105020.
45. Ihara, N., Matsushita, T. Effect of flux creep on irreversibility lines in superconductors. *Physica* C **1996**, *257*, 223–231.
46. Matsushita, T., Otabe, E. S., Wada, H., Takahama, Y., Yamauchi, H. Size dependencies of the peak effect and irreversibility field in superconducting Sm-123 powders. *Physica* C **2003**, *397*, 38–46.
47. Santosh, M., Koblischka, M. R. Experimenting with a superconducting levitation train. *Eur. J. Phys. Educ.* **2014**, *5*(4), 1–9.
48. Lévêque, J., Berger, K., Douine, B. Superconducting Motors and Generators. In: High Temperature Superconductors: Synthesis, Occurence and Applications, eds. M. Muralidhar, M. R. Koblischka, NOVA Science Publishers, Commack, NY, Chap. 12, pp. 263-290 (2018).
49. Fujishiro, H., Tateiwa, T., Fujiwara, A., Oka, T., Hayashi, H. Higher trapped field over 5 T on HTSC bulk by modified pulsed field magnetizing. *Physica* C **2006**, *445-448*, 334–338.
50. Ainslie, M. D., Mochizuki, H., Fujishiro, H., Zhai, W., Namburi, D. K., Shi, Y., Zou, J., Dennis, A. R., Cardwell, D. A. Pulsed Field Magnetization of Single-Grain Bulk YBCO Processed From Graded Precursor Powders. *IEEE Trans. Appl. Supercond.* **2016**, *26*, 6800104.
51. Montminy, M. D., Tannenbaum, A. R., Macosko, C. W. The 3D structure of real polymer foams. *J. Colloid Interface Sci.* **2004**, *280*, 202–211.
52. Nie, Zh., Lin, Y., Tong, Q. Modeling structures of open cell foams. *Comput. Mater. Sci.* **2017**, *131*, 160–169.